Biophotovoltaics

DOI: 10.1002/anie.201303671

Combination of A Photosystem 1-Based Photocathode and a Photosystem 2-Based Photoanode to a Z-Scheme Mimic for Biophotovoltaic Applications**

Tim Kothe, Nicolas Plumeré, Adrian Badura, Marc M. Nowaczyk, Dmitrii A. Guschin, Matthias Rögner, and Wolfgang Schuhmann**

In photosynthesis, conversion of solar energy into chemical energy follows a Z-scheme, which involves two sequential photoinduced charge separation steps (Figure 1 A). First, upon water splitting at photosystem 2 (PS2), the excited electrons are transferred through an electron transport chain that generates a chemiosmotic potential, which provides the energy for ATP synthesis. Then, at photosystem 1 (PS1), upon light absorption and charge separation, the electrons are transferred via ferredoxin to ferredoxin–$NADP^+$ oxidoreductase for the production of NADPH.

The charge separation processes in the Z-scheme inspired the design of photosynthesis-like systems based on organic and inorganic photosensitizers to convert solar energy into chemical energy.[1] Exploiting the yield in light collection of photosynthetic proteins may further increase the efficiency of solar to chemical energy conversion in semi-artificial devices. Various photobioelectrochemical half-cells based either on PS1[2–4] or PS2[5–7] were suggested. However, until now autonomous solar to chemical energy conversion could not be demonstrated. The electrons provided by PS2 are insufficiently energetic, and PS1-based systems require sacrificial electron donors[4] or an externally applied potential[2] to sustain solar to chemical energy conversion. These limitations may be overcome by the serial coupling of both light excitation steps of PS1 and PS2 in a semi-artificial photosynthesis device (Figure 1 B). In analogy to the natural Z-scheme, PS2 would extract electrons from water, which are then transferred to PS1. The charge separation at PS1 would provide electrons which are energetic enough for H_2 evolution if a suitable catalyst such as a hydrogenase was efficiently coupled to the PS1 reaction,[8] as has been proposed previously[5,9,10] to mimic the last step in the Z-scheme (that is, NADPH synthesis). To achieve maximum yields in solar energy conversion, the energy from the charge separation at PS2, that is, the first step in the Z-scheme, needs to be recovered as well.

Herein, we present the first experimental set-up to serially couple PS2 and PS1. We focus on the generation of electrical energy from the difference in potential between the acceptor side of PS2 and the donor side of PS1 (Figure 1 B), that is, that part which contributes to ATP synthesis in the Z-scheme of

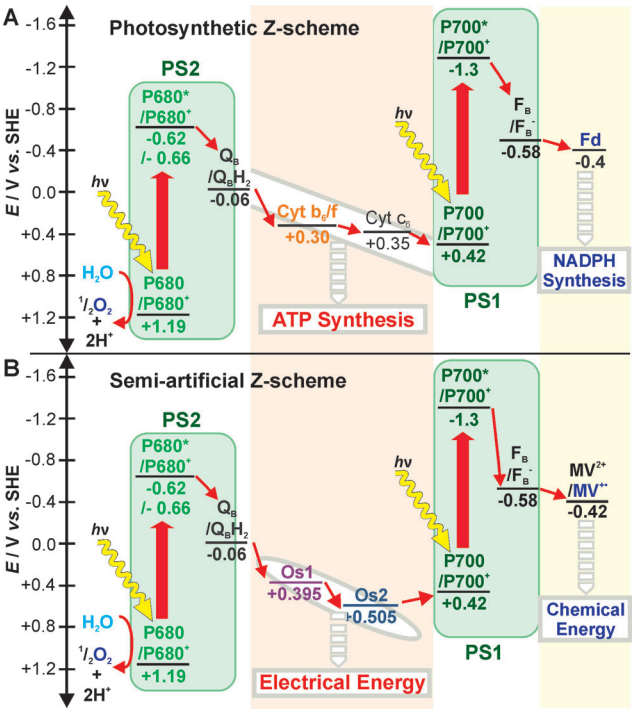

Figure 1. Electron-transfer pathways in the Z-scheme of natural photosynthesis (A) and in the proposed coupled PS2/PS1 system (B): All of the potentials are given versus the standard hydrogen electrode (SHE) in volts (data for the natural Z-scheme according to Refs. [2, 6, 9, 11]). Large red arrows show the light-induced charge separation steps in PS2 and PS1.

[*] T. Kothe, A. Badura, Dr. M. M. Nowaczyk, Prof. Dr. M. Rögner
Plant Biochemistry, Ruhr-Universität Bochum
Universitätsstrasse 150, 44780 Bochum (Germany)
E-mail: matthias.roegner@rub.de
Dr. N. Plumeré, Dr. D. A. Guschin, Prof. Dr. W. Schuhmann
Analytische Chemie—Elektroanalytik & Sensorik and Center for Electrochemical Sciences—CES, Ruhr-Universität Bochum
Universitätsstrasse 150, 44780 Bochum (Germany)
E-mail: wolfgang.schuhmann@rub.de

[**] This work was supported by the EU and the State of NRW in the framework of the HighTech.NRW program (N.P. and W.S.), by the German Federal Ministry for Education and Research, BMBF (M.R.), by the Cluster of Excellence RESOLV (EXC 1069) funded by the Deutsche Forschungsgemeinschaft (T.K., N.P., M.N.N., M.R., and W.S.), and by the COST Action TD1102 Phototech (M.R., N.P. and W.S.).

Supporting information for this article is available on the WWW under http://dx.doi.org/10.1002/anie.201303671.

natural photosynthesis. Our cell is designed to enable the extension of the principle to simultaneous electrical and chemical energy generation (full Z-scheme mimic).

We have previously shown that electrochemical half-cells based on either PS2 or PS1 can be constructed separately: The reducing site of PS2 was contacted to an electrode via an Os-complex modified hydrogel, resulting in high photocurrent densities with unprecedented stability.[6] Similarly, the oxidizing site of PS1 was contacted (again by means of an Os-complex modified redox hydrogel) with an electrode, which resulted in the generation of high cathodic photocurrents.[2] In both cases the same redox polymer was used.

The combination of a PS1-based photocathode and a PS2-based photoanode (Figure 2) results in a photovoltaic cell that operates as a closed system without any sacrificial electron donors or acceptors: Under illumination, water is oxidized to oxygen in the anodic compartment by PS2, and oxygen is reduced in the cathodic compartment by PS1 via methyl viologen (MV); the latter is reduced by PS1 and then regenerated by oxygen reduction, leading finally to water.[12]

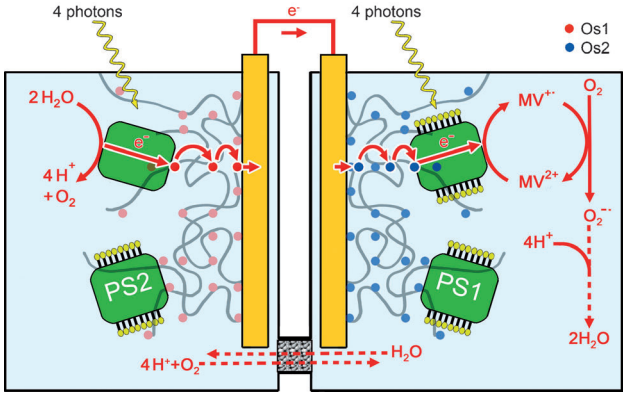

Figure 2. Representation of the proposed biophotovoltaic cell combining a PS2-based photoanode and a PS1-based photocathode. Upon absorption of photons, water molecules are split into electrons and protons. The electrons are transferred to the cathodic half-cell via the outer circuit, where PS1 generates a reductive force of −580 mV vs. SHE and reduces the electron acceptor (methyl viologen). The methyl viologen radical cation is re-oxidized by molecular oxygen, resulting in water as final product.

Notably, the harvest of electrical energy from two coupled light reactions analogous to the Z-scheme in nature (Figure 1) requires different redox potentials of the respective redox hydrogels that wire PS1 and PS2 to their electrodes. The electrical power output of such a photobiovoltaic cell will be determined by 1) the difference in the formal potential of the two redox polymers and 2) the photocurrent density.

The electron-transfer communication between the photoanode and PS2 was achieved with an imidazole-coordinated bispyridyl osmium complex-based redox hydrogel (polymer Os1, formal potential: 395 mV vs SHE). At an applied potential of 500 mV vs. SHE, photocurrent densities of up to 45 $\mu A\,cm^{-2}$ are obtained.[6] At the photocathode, PS1 was immobilized via a pyridine-coordinated bispyridyl osmium complex-based redox hydrogel[13] (polymer Os2) with a more positive formal redox potential of 505 mV vs SHE (for structures of polymer Os1 and Os2, see the Supporting Information). At an applied potential of 200 mV vs. SHE, cathodic photocurrent densities up to 3 $\mu A\,cm^{-2}$ are obtained (see the Supporting Information).

The two-compartment cell with the PS2/Os1-based photoanode and the PS1/Os2-based photocathode allows separate electrolyte and buffer optimization for each protein complex. As the potential of the two redox polymers is almost pH-independent, the difference in pH values between the two compartments should not significantly affect the open-circuit voltage. Electrical connection and illumination of both half-cells generate a steady-state photocurrent of about 1 $\mu A\,cm^{-2}$, which disappears upon switching off the light (Figure 3, left).

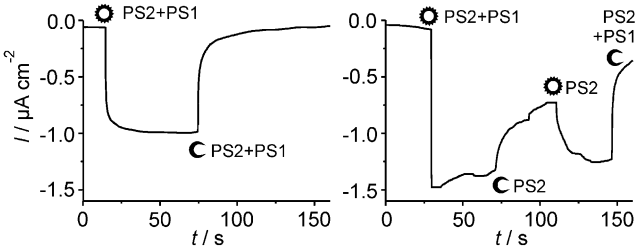

Figure 3. Photocurrent density of the proposed biophotovoltaic cell combining the PS2/Os1-based photoanode and the PS1/Os2-based photocathode as shown in Figure 2. The light status of the respective photoelectrode is indicated by **O** = light on and **C** = light off. Left: Simultaneous illumination of both half-cells with the same light intensity. Right: Starting with the same light intensity on both sides, light at the PS2 half-cell is switched off after 75 s and on again 30 s later. Finally, light was switched off at both half-cells. (Photoanode compartment: buffered electrolyte pH 6.5; photocathode compartment: buffered electrolyte pH 5.5 containing 2 mM methyl viologen.)

Switching off illumination exclusively on the anode side (PS2) results in a decrease of the photocurrent, which could be restored by switching the light on again (Figure 3, right).

To further confirm the contribution of the PS2/Os1-based photoanode to the overall photocurrent, dinoterb (2,4-dinitro-6-*tert*-butylphenol), a herbicide that blocks the Q_B site of the D1 subunit of PS2, was added to the photoanode compartment to deactivate PS2 while both half-cells were continuously illuminated. As shown in the Supporting Information, Figure S3, the photocurrent density substantially decreases upon addition of dinoterb.

To determine the short-circuit current density (I_{SC}), the open-circuit voltage (V_{OC}), and the maximal cell power output (P_{cell}), both photoanode and photocathode were externally connected by a variable resistor. I_{SC} is given by the intersection point of the linear fit of the current density over cell voltage plot and the y axis, and V_{OC} is determined by the intersection point with the x axis (Figure 4). The following values were obtained: $I_{SC} = (2.0 \pm 0.7)\ \mu A\,cm^{-2}$, $V_{OC} = (90 \pm 20)$ mV (Figure 4, left), $P_{cell} = (23 \pm 10)\ nW\,cm^{-2}$ (Figure 4, right). The fill factor (*ff*) is 0.128. The conversion efficiency η for the system, that is, the ratio of power output to power input, is 3.6×10^{-7}, with the maximal power input ($349\ W\,m^{-2}$) resulting from the LEDs used.

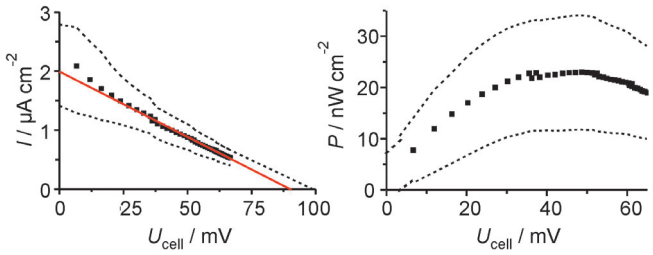

Figure 4. Determination of the short-circuit current density (I_{SC}), the open-circuit voltage (V_{OC}), and the maximal cell power density output (P_{cell}) for the biophotovoltaic cell, combining PS2/Os1-based photoanode and PS1/Os2-based photocathode via an external variable resistor (three experiments with three independently modified electrode pairs; upper and lower limits of the standard deviation given by dashed lines and linear fit given by red line). Left: *I–U* curve. Cell current density, I_{cell}, determined from load and cell potential U_{cell}. Right: *P–U* curve.

The determined V_{OC} correlates with the difference in the formal potentials of the two redox hydrogels Os1 and Os2, while the maximum current density of the complete photovoltaic cell is limited by the PS1/Os2-based photocathode. Thus, the photocurrent density of the PS1/Os2 half-cell in combination with the relatively low potential difference between the two redox hydrogels limits at this stage the performance of the biophotovoltaic cell.

However, the main goal was to proof the feasibility of connecting a PS2-based photoanode and a PS1-based photocathode in a Z-scheme-analogue setup. In future, polymer design for a better electron transfer to PS1 may enable an increased current density by up to one or two orders of magnitude.[2] Additionally, an enhancement in power density can be achieved by higher PS1 and/or PS2 loadings using for example, nanostructured electrode surfaces.[14,15] Furthermore, the potential difference between the polymer-tethered redox species may be tuned and optimally adapted to PS1 or PS2. While the potential of the redox polymer Os2 at the photocathode matches well with PS1, the redox polymer used with PS2 could be about 400 mV more negative to match the potential of the acceptor site of PS2 (Figure 1). This would enable a significant increase in cell voltage and power density.

In conclusion, we have shown the serial coupling of two independent processes of light capturing by PS2 and PS1 yielding a fully closed and autonomous biophotovoltaic cell. This is fundamentally different from previously reported biophotovoltaic devices,[14,16] as it provides the basis for the future use of this "biobattery" in combination with various catalysts: The very reactive electrons may be used for chemical energy conversion instead of reducing oxygen by methyl viologen. Notably, the separation of the oxygen evolving PS2 photoanode from the PS1 photocathode opens the possibility to couple PS1 with oxygen-sensitive biocatalysts such as nitrogenases, CO_2 reducing enzymes of the Calvin cycle, or hydrogenases for the production of biohydrogen.[10] In future, this principle will allow the full energetic exploitation of the photosynthetic Z-scheme in a single setup.

Experimental Section

On the cathode side, an intact trimeric PS1 complex was used, which had been isolated from the thermophilic cyanobacterium *Thermosynechococcus elongatus*; this complex (size 1068 kDa) preserves all subunits and routinely shows a high photochemical (oxygen consumption) activity of about 1000 µmol O_2 per min per mg chlorophyll. Preparation of the PS1 complex was carried out according to Ref. [17]. Dimeric PS2 complexes composed of 20 different subunits[18] and with an average oxygen-evolving activity of about 5000 µmol O_2 per hour per mg chlorophyll[19] were isolated from *Thermosynechococcus elongatus* according to Ref. [20]. Synthesis of the osmium complex-modified polymers Os1 and Os2 is given in the Supporting Information.

Gold disk electrodes (diameter 2 mm) were modified with PS2 and the osmium complex-modified redox polymer Os1 as reported previously.[6] Gold disk electrodes (diameter 2 mm) modified with PS1 integrated into the redox hydrogel Os2 were prepared as follows: A 5 µL droplet containing 10 µg µL^{-1} Os2 and 2 µg µL^{-1} PS1 was placed onto the electrode surface. After drying overnight at 4 °C, the modified electrodes were pre-incubated for 1 h in a sodium citrate buffer (pH 5.5) containing 10 mM $MgCl_2$, 10 mM $CaCl_2$, and 3 mM 1,10 dimethyl-4,4-bipyridinium (methyl viologen).

Photocurrent measurements were carried out in a two-compartment, two-electrode set-up. The anode compartment with the PS2-modified electrode consisted of a glass cuvette filled with buffered electrolyte (MES) pH 6.5 containing 10 mM $MgCl_2$ and 10 mM $CaCl_2$. The cathode compartment with the PS1 modified electrode contained sodium citrate (pH 5.5) buffer with 10 mM $MgCl_2$, 10 mM $CaCl_2$, and 3 mM methyl viologen. Both cuvettes (inner diameter: 2.5 cm; height: 6 cm) were filled with 5 mL of electrolyte and were connected by a salt bridge.

Photocurrent measurements were done with a manually regulated halogen lamp at maximal power output. Evaluation of short-circuit current density (I_{SC}), open-circuit voltage (V_{OC}), maximal cell power output (P_{cell}), fill factor (*ff*), and conversion efficiency (η) was carried out with two light-emitting diodes with a maximum light output at 685 nm and maximum power output of 349 W m^{-2}. In this case, photoanode and photocathode were connected by an external load with 1 kΩ steps from 0 to 3.9 MΩ. Upon increasing the external load stepwise, the cell voltage was measured with a potentiostat. The cell current was calculated with Ohm's law from the measured cell voltage and the given external load. By plotting I_{cell} vs. U_{cell}, I_{SC}, and V_{OC} are derived as the intercept of the linear fit with *y* axis and *x* axis, respectively. These data were used to calculate the maximal power density output of the system. Both current density and power density calculations are based on the surface area of one of the biophotoelectrodes (0.0314 cm^2). The efficiency calculation is based on the total surface area of the electrodes (0.0628 cm^2), as both are illuminated.

Received: April 30, 2013
Revised: July 13, 2013
Published online: November 7, 2013

Keywords: biophotoelectrodes · photosystem 1 · photosystem 2 · redox hydrogels · Z-scheme

[1] a) W. Schuhmann, H.-P. Josel, H. Parlar, *Angew. Chem.* **1987**, *99*, 264–266; *Angew. Chem. Int. Ed. Engl.* **1987**, *26*, 241–243; b) E. S. Andreiadis, M. Chavarot-Kerlidou, M. Fontecave, V. Artero, *Photochem. Photobiol.* **2011**, *87*, 946–964; c) K. Kalyanasundaram, M. Graetzel, *Curr. Opin. Biotechnol.* **2010**, *21*, 298–310.

[2] A. Badura, D. Guschin, T. Kothe, M. J. Kopczak, W. Schuhmann, M. Rögner, *Energy Environ. Sci.* **2011**, *4*, 2435–2440.

[3] O. Yehezkeli, O. I. Wilner, R. Tel-Vered, D. Roizman-Sade, R. Nechushtai, I. Willner, *J. Phys. Chem. B* **2010**, *114*, 14383 – 14388.
[4] N. Terasaki, N. Yamamoto, T. Hiraga, Y. Yamanoi, T. Yonezawa, H. Nishihara, T. Ohmori, M. Sakai, M. Fujii, A. Tohri, M. Iwai, I. Enami, Y. Inoue, S. Yoneyama, M. Minakata, *Angew. Chem.* **2009**, *121*, 1613 – 1615; *Angew. Chem. Int. Ed.* **2009**, *48*, 1585 – 1587.
[5] A. Badura, B. Esper, K. Ataka, C. Grunwald, C. Wöll, J. Kuhlmann, J. Heberle, M. Rögner, *Photochem. Photobiol.* **2006**, *82*, 1385 – 1390.
[6] A. Badura, D. Guschin, B. Esper, T. Kothe, S. Neugebauer, W. Schuhmann, M. Rögner, *Electroanalysis* **2008**, *20*, 1043 – 1047.
[7] M. Kato, T. Cardona, A. W. Rutherford, E. Reisner, *J. Am. Chem. Soc.* **2012**, *134*, 8332 – 8335.
[8] C. E. Lubner, A. M. Applegate, P. Knorzer, A. Ganago, D. A. Bryant, T. Happe, J. H. Golbeck, *Proc. Natl. Acad. Sci. USA* **2011**, *108*, 20988 – 20991.
[9] A. Badura, T. Kothe, W. Schuhmann, M. Rögner, *Energy Environ. Sci.* **2011**, *4*, 3263 – 3274.
[10] S.-O. Wenk, D.-J. Qian, T. Wakayama, C. Nakamura, N. Zorin, M. Rögner, J. Miyake, *Int. J. Hydrogen Energy* **2002**, *27*, 1489 – 1493.
[11] a) J. P. McEvoy, J. A. Gascon, V. S. Batista, G. W. Brudvig, *Photochem. Photobiol. Sci.* **2005**, *4*, 940 – 949; b) T. Shibamoto, Y. Kato, M. Sugiura, T. Watanabe, *Biochemistry* **2009**, *48*, 10682 – 10684; c) S. Veit, K. Takeda, Y. Tsunoyama, D. Rexroth, M. Rögner, K. Miki, *Acta Crystallogr. Sect. D* **2012**, *68*, 1400 – 1408.
[12] R. N. F. Thorneley, *Biochim. Biophys. Acta Bioenerg.* **1974**, *333*, 487 – 496.
[13] D. A. Guschin, Y. M. Sultanov, N. F. Sharif-Zade, E. H. Aliyev, A. A. Efendiev, W. Schuhmann, *Electrochim. Acta* **2006**, *51*, 5137 – 5142.
[14] A. Mershin, K. Matsumoto, L. Kaiser, D. Yu, M. Vaughn, M. K. Nazeeruddin, B. D. Bruce, M. Graetzel, S. Zhang, *Sci. Rep.* **2012**, *2*, 1 – 7.
[15] M. Sosna, L. Stoica, E. Wright, J. D. Kilburn, W. Schuhmann, P. N. Bartlett, *Phys. Chem. Chem. Phys.* **2012**, *14*, 11882.
[16] a) O. Yehezkeli, R. Tel-Vered, J. Wasserman, A. Trifonov, D. Michaeli, R. Nechushtai, I. Willner, *Nat. Commun.* **2012**, *3*, 742; b) D. Gerster, J. Reichert, H. Bi, J. V. Barth, S. M. Kaniber, A. W. Holleitner, I. Visoly-Fisher, S. Sergani, I. Carmeli, *Nat. Nanotechnol.* **2012**, *7*, 673 – 676; c) N. Plumeré, *Nat. Nanotechnol.* **2012**, *7*, 616 – 617.
[17] E. El-Mohsnawy, M. J. Kopczak, E. Schlodder, M. Nowaczyk, H. E. Meyer, B. Warscheid, N. V. Karapetyan, M. Rögner, *Biochemistry* **2010**, *49*, 4740 – 4751.
[18] M. M. Nowaczyk, K. Krause, M. Mieseler, A. Sczibilanski, M. Ikeuchi, M. Rögner, *Biochim. Biophys. Acta Bioenerg.* **2012**, *1817*, 1339 – 1345.
[19] N. Grasse, F. Mamedov, K. Becker, S. Styring, M. Rogner, M. M. Nowaczyk, *J. Biol. Chem.* **2011**, *286*, 29548 – 29555.
[20] H. Kuhl, *J. Biol. Chem.* **2000**, *275*, 20652 – 20659.

